Assessing the Accuracy of Spatial Normalization of Diffusion Tensor Imaging Data in the Presence of Image Artifacts

A. Orlichenko[1], R. J. Dawe[2], H. Peng[2], and K. Arfanakis[2]
[1]Electrical and Computer Engineering, Illinois Institute of Technology, Chicago, IL, United States, [2]Biomedical Engineering, Illinois Institute of Technology, Chicago, IL, United States

Introduction: Diffusion tensor imaging (DTI) is a non-invasive MR imaging technique that can be used to probe in-vivo the microstructural properties of brain tissue [1]. Accurate inter-subject spatial normalization of DTI data is crucial for voxel-based comparisons of neuronal structural integrity [2] and brain connectivity [3] across populations, as well as for the development of a white matter atlas [4]. The purpose of this work was to assess the effects of image artifacts on the accuracy of spatial normalization of DTI data.

Materials and Methods: *(MRI Scans)* Ten normal subjects (30+-5 years of age, 20-40 years of age, 8 male, 2 female) participated in this study. DTI data with minimal artifacts were obtained with Turboprop-DTI, and data with field-inhomogeneity-related artifacts were acquired with SE-EPI-DTI on a 3T GE scanner (General Electric, Waukesha, WI). The parameters for the Turboprop-DTI sequence were: TR=5secs, TE=94msecs, 16 k-space blades, FOV=24x24cm, 256x256 image matrix, 36 contiguous axial slices, and 3.5mm slice thickness. Diffusion weighted (DW) images of each slice were acquired using a minimum energy diffusion encoding scheme with 12 gradient directions and b=900sec/mm^2. Two images with no diffusion weighting (b=0sec/mm^2) were also acquired at the beginning of each scan. The scan time for Turboprop-DTI was 18 minutes and 55 seconds. Most parameters for SE-EPI-DTI were identical to Turboprop-DTI, except that TR=5.4secs, TE=71.8msecs, 8 copies of the b=0sec/mm^2 images and 4 copies of each DW image were obtained. The scan time for SE-EPI-DTI was 5 minutes and 2 seconds, and was selected such that the signal to noise ratio in the raw SE-EPI-DTI data was similar to that in the Turboprop-DTI data. Each subject was also scanned with a 2D gradient-echo sequence with two echoes having TE_1=5msecs, TE_2=11.8msecs, TR=2secs, FOV=24x24cm, 36 contiguous axial slices, 3.5mm slice thickness, 128x128 image matrix.

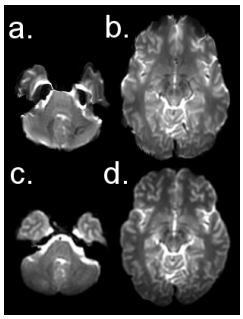

Figure 1. Typical b=0 sec/mm^2 images from corrected SE-EPI-DTI (a-b) and Turboprop-DTI (c-d) data of a subject.

(Data Analysis) Distortions stemming from eddy-currents were corrected in the SE-EPI-DTI data of each subject by registering all DW volumes to the mean DW volume. Phase maps produced from the 2D gradient-echo images were used to correct field inhomogeneity-related distortions in the SE-EPI-DTI data. Further processing was carried out to remove skull and noise outside of the brain in SE-EPI-DTI and Turboprop-DTI datasets. Diffusion tensors were then estimated for both groups of data. A population-based methodology [5] was employed to spatially transform each group of DTI data to the corresponding average space of the population. In this process, each dataset in a group was registered to every other dataset, and the average of these transformations was used to transfer the dataset into population space. Individual registrations were carried out by a piecewise-affine registration algorithm with millions of degrees of freedom and explicit optimization of tensor orientation (DTI-TK, University of Pennsylvania, PA) [6]. Assessment of spatial normalization accuracy for the two groups of DTI data was performed by means of the coherence of primary eigenvectors in white matter [7].

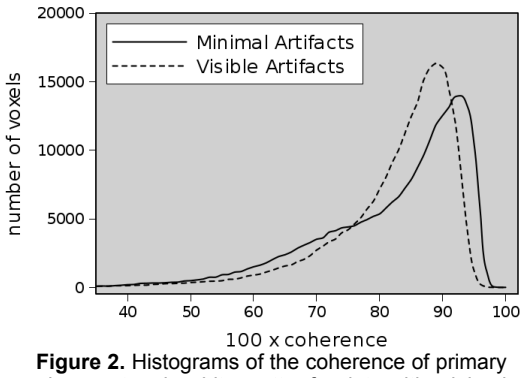

Figure 2. Histograms of the coherence of primary eigenvectors in white matter for data with minimal (solid curve) and visible (dotted curve) artifacts.

Results and Discussion: Residual susceptibility artifacts were present in the corrected SE-EPI-DTI data (Fig.1.a,b). No visible artifacts were included in the Turboprop-DTI data (Fig.1.c,d). Histograms of coherence values in white matter demonstrated that normalization of datasets with minimal artifacts resulted in relatively more white matter voxels with high coherence values, than data with visible artifacts (Fig.2). Higher coherence values suggest improved matching of the primary eigenvector of diffusion tensors across subjects. Moreover, maps of the coherence for the two groups of data showed that the greatest differences in coherence occurred in major white matter structures throughout the brain (Fig.3). Table 1 shows significant differences in coherence values of 3 white matter structures when using data with minimal and visible artifacts. Therefore, it was concluded that data with minimal artifacts increase the accuracy of spatial normalization in DTI. Finally, the amount of artifacts included in SE-EPI-DTI data varies for different subjects, and different imaging parameters (e.g. slice thickness, TE, acceleration factor for parallel imaging, etc.). However, the purpose of this work was not to compare the two acquisition sequences and different imaging parameters, but to evaluate the effects of artifacts on the accuracy of spatial normalization. Data with more severe artifacts than those in the corrected SE-EPI-DTI data used here is expected to further reduce the accuracy of spatial normalization, while data with fewer artifacts is expected to produce coherence values that are more similar to those obtained for the Turboprop-DTI data.

	Coherence for data with minimal artifacts	Coherence for data with visible artifacts	p-value
Genu	0.922 ± 0.019	0.903 ± 0.016	< 3x10^{-7}
Splenium	0.944 ± 0.011	0.929 ± 0.007	< 10^{-20}
Internal Capsule	0.936 ± 0.016	0.926 ± 0.013	.002

Table 1. Mean and standard deviation of the coherence of primary eigenvectors in selected white matter regions. Two-tailed t-tests were used to assess the significance of any differences. Only differences with p<0.01 were considered significant.

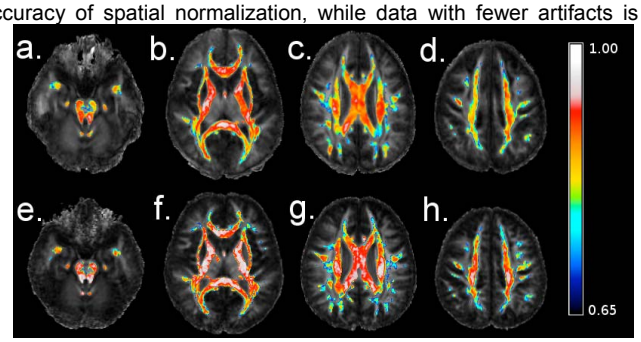

Figure 3. Maps of the coherence of primary eigenvectors for data with visible (a-d) and minimal (e-h) artifacts, overlayed on fractional anisotropy maps derived from the mean tensors of each group of data.

References: [1] Basser PJ et al., *Journal of Magnetic Resonance* 1996;111:209-219. [2] Le Bihan D et al., *Journal of Magnetic Resonance Imaging* 2001;13:534-546. [3] Basser PJ et al., *Magnetic Resonance in Medicine* 2000;44:625-632. [4] Mori S et al., *NeuroImage* 2008;40:570-582. [5] Van Hecke W et al., *NeuroImage* 2008;43:69-80. [6] Zhang H et al., *Medical Image Analysis* 2006;10:764-785. [7] Alexander DC et al., *IEEE Transactions on Medical Imaging* 2001;20:1131-1139.